Beyond the gain exponent: Effect of damping, scale length, and speckle length on stimulated scatter

R. L. Berger,[1,*] L. J. Suter,[1] L. Divol,[1] R. A. London,[1] T. Chapman,[1] D. H. Froula,[2] N. B. Meezan,[1]
P. Neumayer,[3] and S. H. Glenzer[4]

[1]*Lawrence Livermore National Laboratory, University of California, P.O. Box 808, Livermore, California 94551, USA*
[2]*Laboratory for Laser Energetics, University of Rochester, 250 East River Road, Rochester, New York 14623-1299, USA*
[3]*ExtreMe Matter Institute EMMI, GSI Helmholtzzentrum für Schwerionenforschung, Planckstrae 1, 64291 Darmstadt, Germany*
[4]*SLAC National Accelerator Laboratory, 2575 Sand Hill Road, MS 72 Menlo Park, California 94025, USA*

Three-dimensional wave propagation simulations and experiments show that the gain exponent, an often used metric to assess the likelihood of stimulated Brillouin scatter, is insufficient and must be augmented with another parameter, N_r, the ratio of the resonance length, L_{res}, to the laser speckle length. The damping rate of ion acoustic waves, ν, and thus L_{res}, which is proportional to ν, are easily varied with plasma species composition, e.g., by varying the ratio of hydrogen and carbon ions. As N_r decreases, stimulated Brillouin scattering increases despite the same gain exponent.

PACS number(s): 52.57.−z, 52.35.Mw, 52.38.−r, 52.65.−y

Ideal performance of indirect drive inertial confinement fusion (ICF) at the National Ignition Facility (NIF) [1] assumes laser backscatter losses are insignificant, but losses as high as 10% can be accommodated with appropriate hohlraum and laser design choices. Stimulated Brillouin backscatter (SBS), the process in which an ion acoustic wave (IAW) reflects a portion of the laser light back and subsequently amplifies the same ion wave in an unstable loop, has the added concern that expensive optical components can be damaged. Replacement of components not only adds to the facility costs but also reduces the shot rate.

The standard ICF hohlraum design consists of a gold or uranium cylinder ∼1 cm long and ∼0.6 cm in diameter, with laser entrance holes (LEHs) at each end through which 192 beams are directed at the walls. The interior of the hohlraum is filled with helium (He), hydrogen (H), or a HeH mixture for ignition designs with a deuterium-tritium filled capsule. Experiments are also done with hydrocarbon gas fills for laser propagation studies.

By design [2,3], the low charge state (Z) of the fill gas absorbs a small fraction of the laser power while the high-Z plasma absorbs the laser power and efficiently converts it to x radiation that drives the capsule ablation. The high-Z plasma ablated from the wall (the gold bubble) has a charge state $Z_{au} \sim 60$, and a length $L \sim C_s t_p \lesssim 0.5$–1 mm, where $C_s \sim 3 \times 10^7$ cm/s is the sound speed and $t_p \sim 2$–3 ns is the time measured from the beginning of peak laser power. The threshold for significant SBS depends on the Landau damping rate of the IAW, ν, which itself depends on the number of ions at the IAW phase velocity, $v_{ph} = \omega/k$, where ω and k are the frequency and wave number, respectively. In a single ion species plasma, that number depends only on ZT_e/T_i. Thus, the IAW is strongly Landau damped ($\nu/\omega \gtrsim 0.1$) in the He fill gas but weakly damped in the high-Z plasma ($\nu/\omega \sim 0.006$). The high-Z IAW damping rate can be increased significantly by adding a light ion [4] because the phase velocity is determined by the high-Z ions but the Landau damping by

the light ions such as boron ($Z = 5, A = 11$), as shown in Table I.

In this Rapid Communication, we reexamine the data of Ref. [5] and show with new three-dimensional simulations and analysis that additional physics "beyond" the gain exponent alone is required to quantitatively model SBS. Another parameter—ν itself or $N_r (\propto \nu)$, the ratio of the resonance length to the laser speckle length—is also important. The speckle length and width are $l_{sp} \sim 5$–$8 f^2 \lambda_0$ and $l_\perp = f \lambda_0$, respectively, where f is the f number of the lens and λ_0 is the laser wavelength. The result of the experiments and the three-dimensional (3D) simulations that reproduce these results and highlight the effect of the damping rate are shown in Fig. 1. The 3D simulations with pF3D [6–8], include self-consistently the light wave's speckle properties and the plasma parameters from hydrodynamic simulations. Note the ∼50% increase in the threshold for SBS as ν/ω increases from 0.045 to 0.2. Table I shows that NIF hohlraums have regions where $L_{res} \ll l_{sp}$ in the gold bubble as well as the opposite limit $L_{res} \gg l_{sp}$ in the gas fill; thus, a more sophisticated analysis of relevant experimental data by including new physics has high impact [9].

ICF experiments have relied on gain analyses to interpret experimental results and guide hohlraum design [2,10] with the expectation that small backscatter would occur if the gain were small enough. The gain is given by $G(k,\omega) = \int_z dz \, \kappa(k,\omega,z)$ with gain rate $\kappa = (k^2 v_0^2/4c^2 k_s) \text{Im}[\chi_e(1 + \chi_i)/\varepsilon]$ and $\varepsilon = 1 + \chi_i + \chi_e$ is the plasma wave dispersion function [11]. Here, ω_0 is the laser light frequency, $v_0 = eE_0/(m_e\omega_0)$ is the jitter velocity of an electron in the laser electric field $E_0 (\propto \sqrt{I_L})$, I_L is the laser intensity, c is the speed of light, and k_s is the SBS light wave number. When the acoustic wave is driven on resonance, $\text{Re}[\varepsilon(k,\omega)] = 0$, $\text{Im}[\varepsilon(k,\omega)] \propto \nu$, such that $\kappa \propto \nu^{-1}$. Because the flow velocity varies in space, resonance is only maintained over the resonance length $L_{res} = (\nu/\omega)L_{V_z}$, where $L_{V_z} = C_s/|\partial V_z/\partial z|$ is the gradient scale length of the plasma flow velocity, V_z, along the laser light propagation direction. Thus, $G(k,\omega) \sim \max(\kappa)L_{res}$ is independent of the damping rate. If gain is the same and the only metric, SBS that occurs over several millimeters in the gas fill with strong IAW damping presents the same risk as SBS that occurs over a less

*berger5@llnl.gov

TABLE I. OMEGA/NIF mixed species plasmas properties.

OMEGA gas fill[a]			NIF gold bubble[b]			NIF gas fill[c]		
f_H[d]	ν/ω	L_{res} (mm)	f_B[e]	ν/ω	L_{res} (mm)	Gas	ν/ω	L_{res} (mm)
0.04	0.03	0.09	0	0.006	0.006	C	0.02	0.28
0.17	0.045	0.14	0.2	0.02	0.02	CH	0.1	1.4
0.26	0.08	0.24	0.4	0.04	0.04	He	0.15	2.1
0.74	0.2	0.6	0.8	0.07	0.08	HeH	0.35	5
f-no.	l_{sp} (mm)		f-no.	l_{sp} (mm)		f-no.	l_{sp} (mm)	
6.7	0.08		8	0.12		8	0.12	

[a]$T_e = 2.5$ keV, $T_i = 0.4$ keV, $n_e/n_c = 0.06$.
[b]$T_e = 3.5$ keV, $T_i = 1.5$ keV, $n_e/n_c = 0.1$.
[c]$T_e = 2.6$ keV, $T_i = 1.5$ keV, $n_e/n_c = 0.07$.
[d]Fraction of hydrogen.
[e]Fraction of boron.

than 1 mm in the gold bubble with weak IAW damping [12]. Neumayer [5] reported experimental results with mixtures of CO_2 ($\nu/\omega \gtrsim 0.01$) and CH_4 ($\nu/\omega \gtrsim 0.1$) gases that appeared to support this view. Here, we show that the deviations from that scaling are resolved by including more detailed physics made possible by 3D simulations that include the variation in resonance length as the damping rate is varied.

Although SBS has been measured from NIF hohlraums at levels of up to 30% over intervals of ∼1 ns, the results depend on the amount of cross-beam power transfer [13], the duration of peak power, and the density of the initial He fill gas. In addition, beams propagate through several materials (He and CH or carbon ablated from the capsule for some beams; He and gold for other beams) with complex interfaces and velocity
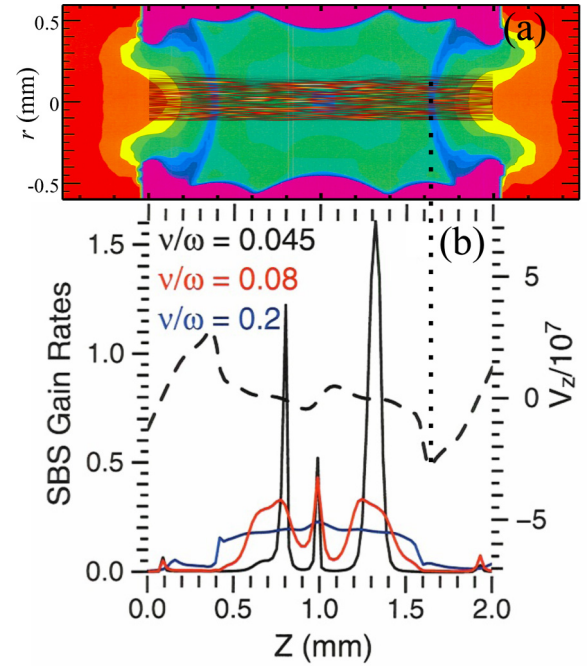

FIG. 2. (Color online) (a) This figure shows the "interaction" laser beam propagating along the axis of a gas-filled hohlraum overlaid on an electron density image of a hohlraum from HYDRA simulations. The 33 heater beams (not shown) are directed at the inside of the hohlraum wall (shown in purple). (b) The plasma velocity along the hohlraum axis (dashed line) and, for $\nu/\omega = 0.045, 0.08, 0.2$, the SBS gain rates normalized such that the gains (the integral of the rates) are equal. The velocity bump in the dashed curve is associated with the peak density of a "blast" wave as indicated by the vertical dotted line.

gradients, all of which make simulation of the NIF results difficult to interpret. Neumayer's experiments [5] provide a good data set to test our modeling capability and to identify the essential parameters that control SBS.

Neumayer's experiment was one of a number of experiments to address the understanding of laser propagation in NIF conditions that were done on the OMEGA laser facility, e.g., Refs. [5,14–16]. Thirty-three beams (1 ns, 400 J each) are directed at the inside gold walls of the hohlraum to heat the low-Z gas and gold plasma. At a time 300 ps after the heater beams begin, an "interaction" beam, which has little effect on plasma parameters, is directed down the axis of the hohlraum. An image of an OMEGA gas-filled hohlraum from HYDRA [17] simulations with the interaction laser beam superimposed is shown in Fig. 2(a).

In this Rapid Communication, the experimental and simulation results presented in the figures are distinguished by the IAW damping rate, ν/ω. The plasma composition—the gas mixtures—are labeled by the hydrogen fraction, f_H, the ratio of the number of hydrogen atoms to the sum of all atoms. The relation of ν/ω to f_H is given in Table I. Smaller values of f_H have smaller ν/ω. The experiments with $\nu/\omega \leqslant 0.08$ used a phase plate that produced a 200 μm circular spot in the plasma with an $f/6.7$ lens [5]. The laser power, approximately constant with a 1 ns pulse length, was varied between 100 and 400 GW. A laser power of 100 GW corresponds to a
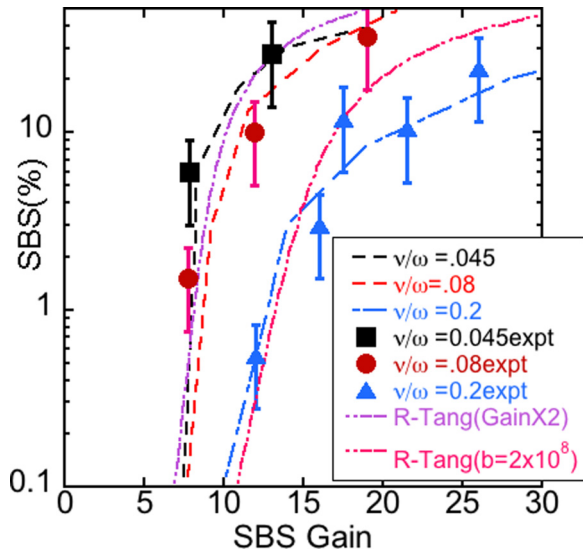

FIG. 1. (Color online) The SBS reflectivity is shown as a function of the calculated gain for both experiments and pF3D simulations. The results for different ν/ω are denoted with different colors. The symbols with error bars represent the SBS measured at OMEGA in hohlraum experiments. The dashed lines are pF3D calculations of the level of backscatter. The purple and magenta dash-dotted curves are results from Eq. (3) with the gain multiplied by 2 and $b = 1 \times 10^{-9}$ and with the nominal gain and $b = 2 \times 10^{-8}$.

spot-average intensity of $I_L = 2.2 \times 10^{14}$ W/cm^2. The data with $\nu/\omega = 0.2$ had an IAW damping too large and a gain too small to produce significant SBS for $I_L < 1 \times 10^{15}$ W/cm^2, that is, a gain less than 10. Thus, a phase plate was used that produced a 100 μm focal spot with $I_L \lesssim 4 \times 10^{15}$ W/cm^2.

The velocity profile along the hohlraum axis, shown in Fig. 2(b), varies slightly and nearly linearly over the central 1 mm of the profile where most of the SBS occurs in the pF3D simulations. The hydrodynamic simulations show that the axial flow velocity, the electron temperature, and the electron density are sensitive neither to the hydrogen fraction nor to the intensity and energy of the interaction beam. In Fig. 2(b), examples of the gain rate for weakly and strongly damped IAWs but the same total gain are shown. As ν/ω decreases, the interaction takes place over a shorter resonance length, L_{res}. The velocity gradients within the plateau region are unimportant if the damping rate exceeds the magnitude of the Doppler shift excursion, that is, if $\nu/\omega > 2k_0|\Delta V_z|/\omega \sim 0.15$. Table I lists ν/ω and L_{res} for the various gas mixtures, found by solving the kinetic IAW dispersion relation [4] From Fig. 2(b), it is clear for $\nu/\omega \lesssim 0.045$ that there are in fact separate gain regions each not much longer than the length of one 351 nm laser speckle. For $\nu/\omega = 0.2$, the gain rate is almost uniform over the central 1 mm of the plasma. In this case, the gain per speckle is ~ 1 when the measured SBS is $\sim 1\%$, and the amplification takes place over many speckle ranks, that is, over many $N_{\mathrm{rank}} = L/l_{\mathrm{sp}}$, where L is the plasma size. For strong damping and weak velocity gradients, L, in this case the length of the density plateau determines the gain such that [18]

$$G = 2\frac{\gamma_0^2}{\nu v_g}\min\left(L, 2\pi L_{\mathrm{res}}\right), \tag{1}$$

$$\gamma_0^2 = \frac{1}{16}\frac{n_e}{n_c}\frac{v_0^2}{v_e^2}\omega_0\omega. \tag{2}$$

In Eqs. (1) and (2), v_e is the electron thermal velocity, γ_0 is the SBS growth rate in the absence of damping, and $v_g = c^2 k_s/\omega_s$ is the group velocity of the SBS light. OMEGA [19] and NIF [20] use continuous phase plates that produce well-characterized laser beam spots at focus by introducing transverse phase nonuniformities in the near field. Although the laser intensity is smooth on the large focal-spot scale, it consists of a distribution of intense small scale speckles of mean intensity I_0 and a variance equal to I_0. Thus a significant fraction of the laser power has local intensity more than twice the mean. At the OMEGA laser, $l_{\mathrm{sp}} \sim 0.08 - 0.12$ mm as $f = 6.7$ and $\lambda_0 = 351$ nm. At the NIF, $f = 8$ and $l_{\mathrm{sp}} \sim 0.11$–$0.18$ mm. The distribution of speckle intensity follows an exponential decrease, e.g., $F(I) \sim \exp(-I/I_0)$, for both cases. The smaller spot has four speckles with $I_{\mathrm{sp}} > 10I_0$; the larger has 25. The millimeter scale NIF spots have hundreds.

If $N_r \gg 1$, SBS averages over the small scale hot spots with total reflectivity that is a function of I_0. In the other limit $N_r \ll 1$, the averaging is incomplete and a higher reflectivity is expected [21] because the more intense speckles can amplify the SBS light several orders of magnitude without depleting a large fraction of their power. As ν/ω decreases, more and more speckles have large enough power to amplify the SBS many
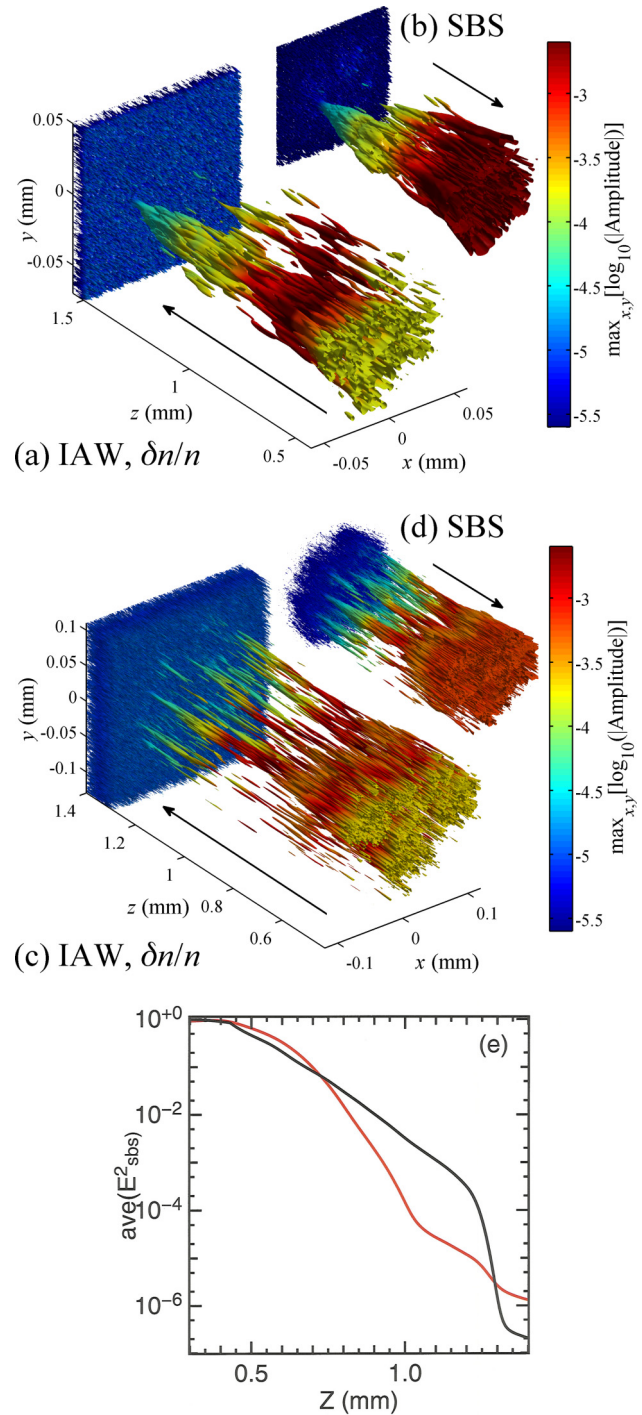

FIG. 3. (Color online) The IAW amplitude ($|\delta n_{ac}/n_c|$) and SBS light intensity (arbitrary units) for cases [(a),(b)] $\nu/\omega = 0.2$ and [(c),(d)] $\nu/\omega = 0.08$. The surface contour shown is at the 10% level everywhere, where the plotted quantities are normalized to the local maximum across the (x-y) plane to account for the exponential amplification. The color provides this actual local maximum. The dark blue region at z $\gtrsim$ 1.4 mm is for IAWs the thermal fluctuation level and for SBS light the Thomson scattering level of the light prior to significant amplification. The line plots (e) show ave(E_{SBS}^2), the reflected light intensity averaged over the transverse area (x and y), for $\nu/\omega = 0.2$ (black) and $\nu/\omega = 0.08$ (red); ave(E_{SBS}^2) is normalized to the maximum value, which is about two times larger for $\nu/\omega = 0.2$ than $\nu/\omega = 0.08$.

orders of magnitude. In this experiment and simulations, the speckle length is fixed while the resonance length is varied by varying ν. The dependence of the reflectivity on N_r can also be demonstrated by varying the speckle length for fixed ν [6] by using $f/3$ and $f/6$ lenses [22].

To quantify the effect of N_r on SBS, we use pF3D to model the 3D propagation and interaction of the laser light with the plasma. By coupling nonlinear hydrodynamics with time and space enveloped light and plasma waves, pF3D includes the evolution of ponderomotive filamentation and forward and backward Brillouin scatter. The simulations use the phase distortions measured for the phase plates in the experiments and plasma parameters from radiation-hydrodynamic simulations. In Fig. 3(a), all the increase of SBS for $\nu/\omega = 0.2$ for $z \gtrsim 1.4$ mm occurs in one large-amplitude speckle with $I_{sp} \sim 10 \times I_0$. The increase is consistent with Eq. (1) with $L = l_{sp}$ and $v_0^2 \propto I_{sp}$. The SBS from that speckle becomes the source for subsequent amplification of IAWs and SBS light over the remainder of the plasma. In contrast, the SBS for $\nu/\omega = 0.08$ originates in a number of speckles near the resonance surface at $z = 1.3$ mm as the isosurface plot of the IAW amplitude in Fig. 3(c) shows. As the SBS light propagates backward through the laser beam, it diffracts, amplifies exponentially, and drives IAWs over a larger and larger cross section of the laser beam. For $\nu/\omega = 0.2$, $|E_{SBS}|^2$ increases exponentially at a constant rate between $z = 1.4$ and $z = 0.4$. That assertion is substantiated by Fig. 3(e), where $\mathrm{ave}(E_{SBS}^2)$, the x-y average intensity of the reflected light, is shown for both cases. For $\nu/\omega = 0.08$, the reader may notice in Figs. 3(c) and 3(d) an increased rate near the resonant surfaces at $z \simeq 1.3, 1.0$, and 0.7 where the red color denoting a maximum of the IAW density fluctuations is pronounced. The length over which the light amplifies exponentially is shorter for $\nu/\omega = 0.08$, between $z = 0.6$ and $z = 1$. However, as shown in Fig. 3(e), $\mathrm{ave}(E_{SBS}^2)$ for $\nu/\omega = 0.08$ increases at a gain rate about twice that for $\nu/\omega = 0.2$ in the region where they are both exponentially increasing. Near $z = 0.5$, the speckled SBS for $\nu/\omega = 0.08$ occupies nearly the same area as the incident laser light spot. Note in the strongly damped case that the SBS and IAW continue to grow until $z = 0.4$ as one expects from the gain rate plotted in Fig. 2(b). For $z < 0.4$, IAWs [shown in Fig. 3(a)] decrease in amplitude and SBS [shown in Fig. 3(b)] no longer grows. In the weakly damped case shown in Figs. 3(c) and 3(d) for the IAW and SBS, respectively, the growth is limited to a smaller length in z, again as one expects from Fig. 2(b).

With use of the "Tang" model [23] for the SBS reflectivity, r, as a function of the gain, G,

$$r = \frac{b \, \exp\left[(1-r)\,G\right]}{(1-r+b)} \tag{3}$$

we generate two curves in Fig. 1 that also model the data well and are motivated by the results in Fig. 3. The curve that

models the strongly damped case uses the nominal gain, $G = G(I_0)$, with an initial seed value for the backscattered light of $b = 2 \times 10^{-8}$. The weakly damped data is modeled well with a "speckle-enhanced" $G = 2G(I_0)$, twice the calculated gain, and with the much smaller initial value, $b = 1 \times 10^{-9}$. The larger initial value for the strongly damped case takes account of the rapid increase in one speckle with ten times the average intensity near $z = 1.4$ mm. If $b = 1 \times 10^{-9}$ were used for $\nu/\omega = 0.2$, the threshold gain for the strongly damped case would be twice that for the weakly damped case in disagreement with pF3D and the data. Thus, the relatively few speckles for the smaller spot when $\nu/\omega = 0.2$ leads to the outsized importance of "hot" speckles, which weakens the scaling of the reflectivity with ν/ω. The SBS reflectivity for $f_H = 0.04$ for which $\nu/\omega = 0.03$ was also measured and can also be modeled with a Tang curve with an effective gain three times the calculated gain. The experimental and simulation results presented in Fig. 1, the main result of this Rapid Communication, are of intrinsic interest and of practical importance to the NIF ignition designs. These results show clearly that the SBS reflectivity depends not only on the gain but also on ν/ω or, equivalently, N_r. Also, one sees from Fig. 1 that the measured and simulated reflectivity increases with gain more slowly as ν/ω increases. When the amplification occurs over many ranks of speckles with a gain per speckle $\lesssim 1$, the gain rate, an average over many speckles, approaches the rate for an idealized uniform laser beam. For $f_H = 0.74$ with about ten ranks of speckles contributing, the threshold gain is ~ 12. For the lower ν/ω, the threshold gain is about 8; for CO_2 plasmas with no added hydrogen, $\nu/\omega \sim 0.01$ and the threshold gain would be lower still. These are the NIF relevant damping rates for SBS in the pure gold plasma region as shown in Table I.

There are at least two important benefits to increasing the damping rate: the gain rate is reduced and the spatial growth is spread over a larger volume, which decreases the effects of the speckles. Spreading the growth over a larger volume ensures against large spikes in backscatter that could occur if long-wavelength hydrodynamic fluctuations produce local regions with long-lived negligible flow velocity gradients.

[1] E. I. Moses and C. R. Wuest, Fusion Sci. Technol. **47**, 314 (2005).

[2] D. E. Hinkel, D. A. Callahan, A. B. Langdon, S. H. Langer, C. H. Still, and E. A. Williams, Phys. Plasmas **15**, 056314 (2008).

[3] N. B. Meezan, L. J. Atherton, D. A. Callahan, E. L. Dewald *et al.*, Phys. Plasmas **17**, 056304 (2010).

[4] E. A. Williams, R. L. Berger, R. P. Drake, A. M. Rubenchik, B. S. Bauer, D. D. Meyerhofer, A. C. Gaeris, and T. W. Johnston, Phys. Plasmas **2**, 129 (1995).

[5] P. Neumayer, R. L. Berger, L. Divol, D. H. Froula, R. A. London, B. J. MacGowan, N. B. Meezan, J. S. Ross, C. Sorce, L. J. Suter, and S. H. Glenzer, Phys. Rev. Lett. **100**, 105001 (2008); P. Neumayer, R. L. Berger, D. Callahan, L. Divol, D. H. Froula, R. A. London, B. J. MacGowan, N. B. Meezan, P. A. Michel, J. S. Ross, C. Sorce, K. Widmann, L. J. Suter, and S. H. Glenzer, Phys. Plasmas **15**, 056307 (2008).

[6] R. L. Berger, B. F. Lasinski, A. B. Langdon, T. B. Kaiser, B. B. Afeyan, B. I. Cohen, C. H. Still, and E. A. Williams, Phys. Rev. Lett. **75**, 1078 (1995); **76**, 3239 (1996).

[7] R. L. Berger, C. H. Still, E. A. Williams, and A. B. Langdon, Phys. Plasmas **5**, 4337 (1998); C. H. Still, R. R. Berger, A. B. Langdon, D. E. Hinkel, L. J. Suter, and E. A. Williams, *ibid.* **7**, 2023 (2000).

[8] L. Divol, R. L. Berger, N. B. Meezan, D. H. Froula, S. Dixit, P. Michel, R. London, D. Strozzi, J. Ross, E. A. Williams, B. Still, L. J. Suter, and S. H. Glenzer, Phys. Plasmas **15**, 056313 (2008).

[9] It is important to emphasize that the spatial growth is not limited to one speckle when the resonance length is greater than a speckle length, rather the effective spatial growth rate is reduced.

[10] D. J. Strozzi, E. A. Williams, D. E. Hinkel, D. H. Froula, R. A. London, and D. A. Callahan, Phys. Plasmas **15**, 102703 (2008).

[11] J. F. Drake, P. K. Kaw, Y. C. Lee, G. Schmidt, C. S. Liu, and M. N. Rosenbluth, Phys. Fluids **17**, 778 (1974).

[12] The strong inverse bremsstrahlung absorption of the laser light by gold limits the interaction to ~0.05 mm.

[13] P. Michel, L. Divol, E. A. Williams, S. Weber *et al.*, Phys. Rev. Lett. **102**, 025004 (2009).

[14] D. H. Froula, L. Divol, R. L. Berger, R. A. London, N. B. Meezan, D. J. Strozzi, P. Neumayer, J. S. Ross, S. Stagnitto, L. J. Suter, and S. H. Glenzer, Phys. Rev. Lett. **101**, 115002 (2008).

[15] D. H. Froula, L. Divol, R. A. London, R. L. Berger, T. Döppner, N. B. Meezan, J. S. Ross, L. J. Suter, C. Sorce, and S. H. Glenzer, Phys. Rev. Lett. **103**, 045006 (2009).

[16] D. H. Froula, L. Divol, R. A. London, R. L. Berger, T. Döppner, N. B. Meezan, J. Ralph, J. S. Ross, L. J. Suter, and S. H. Glenzer, Phys. Plasmas **17**, 056302 (2010).

[17] M. M. Marinak, S. W. Haan, T. R. Dittrich, R. E. Tipton, and G. B. Zimmerman, Phys. Plasmas **5**, 1125 (1998).

[18] J. D. Lindl, P. Amendt, R. L. Berger, S. G. Glendinning, S. H. Glenzer, S. W. Haan, R. L. Kauffman, O. L. Landen, and L. J. Suter, Phys. Plasmas **11**, 339 (2004).

[19] T. R. Boehly, D. Brown, R. Craxton, R. Keck, J. Knauer, J. Kelly, T. Kessler, S. Kumpan, S. Loucks, S. Letzring, F. J. Marshall, R. L. McCrory, S. F. B. Morse, W. Seka, J. M. Soures, and C. P. Verdon, Opt. Commun. **133**, 495 (1997).

[20] S. N. Dixit, M. D. Feit, M. D. Perry, and H. T. Powell, Opt. Lett. **21**, 1715 (1996); C. A. Haynam, P. J. Wegner, J. M. Auerbach, M. W. Bowers, S. N. Dixit, G. V. Erbert, G. M. Heestand, M. A. Henesian, M. R. Hermann, K. S. Jancaitis, K. R. Manes, C. D. Marshall, N. C. Mehta, J. Menapace, E. Moses, J. R. Murray, M. C. Nostrand, C. D. Orth, R. Patterson, R. A. Sacks, M. J. Shaw, M. Spaeth, S. B. Sutton, W. H. Williams, C. C. Widmayer, R. K. White, S. T. Yang, and B. M. Van Wonterghem, Appl. Opt. **46**, 3276 (2007).

[21] H. A. Rose and D. F. DuBois, Phys. Rev. Lett. **72**, 2883 (1994); H. A. Rose, Phys. Plasmas **2**, 2216 (1995).

[22] S. D. Baton, F. Amiranoff, V. Malka, A. Modena, M. Salvati, C. Coulaud, C. Rousseaux, N. Renard, Ph. Mounaix, and C. Stenz, Phys. Rev. E **57**, R4895(R) (1998).

[23] D. W. Forslund, J. M. Kindel, and E. L. Lindman, Phys. Fluids **18**, 1002 (1975); C. L. Tang, J. Appl. Phys. **37**, 2945 (1966).